REFRACTIVITY-FROM-CLUTTER USING GLOBAL ENVIRONMENTAL PARAMETERS

Peter Gerstoft[1], *L. Ted Rogers*[2], *William S. Hodgkiss*[1], *and Galina Rovner*[1]

[1] Marine Physical Laboratory, University of California San Diego, La Jolla, CA 92093-0238 USA

[2] Atmospheric Propagation Branch, SPAWAR Systems Center, San Diego, CA 92152 USA

Abstract-This paper examines the sensitivity of radar clutter returns to variations in parameters used to describe the refractive environment that is associated with surface-based ducts. This supports determining efficient parameters so as to minimize the search space required in the inverse problem of inferring the refractivity environment from observations of radar sea clutter.

First, the sensitivity of replica fields to variations in range-independent parameters are considered. Next, variations in the parameters with range are modeled as a Markov processes. It is seen that either source of variation could explain variations in radar clutter observations obtained during a surface-based ducting event with the 3.0 GHz Space Range Radar (SPANDAR) at Wallops Island, VA.

We then use the Simulated Annealing / Genetic Algorithm (SAGA) general purpose inversion code to infer refractivity parameters from observed clutter. SAGA is configured to use an embedded parabolic equation electromagnetic propagation model, a four-parameter model for atmospheric refractivity, and a linear least-squares objective function. The mismatch between (a) the optimal replica field and the observed clutter and (b) the inferred refractivity profile and the range-dependent refractivity structure obtained by *in situ* measurements, is discussed.

1. INTRODUCTION

Of the non-standard refractivity structures affecting horizontal radar propagation, e.g., sub-refraction, evaporation ducts, etc., the most spectacular effects arise from surface-based ducts [1]. A common meteorological event giving rise to a surface-based duct is a thermal internal boundary layer that forms when warm continental air flows over a cooler ocean, leading to a refractivity structure that resembles the model shown in Fig. 1. Surface-based ducts give rise to effects including clutter rings in the radar's plan position indicator (PPI), height errors for 3-D radar, and contamination of automated rain-rate calculations from weather radars. A wide range of phenomena—from gravity waves to diurnal cycles—affect how the duct structure is realized and accurately estimating the structure over the spatial extent of a radar's coverage is difficult.

The first description of estimating surface-based duct structure from radar clutter observations using modern tools was by Krolik *et al*. [2, 3]. They formulated the refractivity-from-clutter (RFC) problem as a maximum likelihood (ML) problem using a vector of global refractivity parameters and log-amplitude data as obtained from a radar. The work in this paper supports determining which global parameters (which can include parameters describing range-dependency) should be used in RFC.

Funded by the Office of Naval Research Codes 321 and 322.

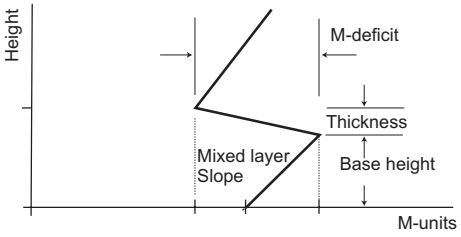

Fig. 1. Tri-linear refractivity model.

1.1. Modeling and inversion

From [4], the clutter power p (in dB) in the absence of receiver noise, can be modeled as

$$p(r, \mathbf{m}) = -40 \log f(r, \mathbf{m}) + 10 \log(r) + C \qquad (1)$$

where f is the one-way propagation loss as modeled using the Terrain Parabolic Equation Model (TPEM) [5]. C is an offset that takes into account radar parameters and the radar sea clutter cross section (σ°). σ° is assumed to be range-independent. Krolik *et al.* found improved results by allowing some compliance for range-dependency in σ°, however, it is not possible yet to draw a general conclusion as to if, or how much compliance is useful. The elements of $\mathbf{m}$ correspond to the four refractivity parameters illustrated in Fig. 1.

Replica vectors are calculated from Eq. (1) to obtain, $\mathbf{p}(\mathbf{m}) = \{p_c(\mathbf{m}, r_1), \cdots, p_c(\mathbf{m}, r_N)\}$. C is adjusted so the average power of the replica vector (dB) has the same average power as the observed clutter power $\mathbf{q}$. As with the radar data, all observed data $\mathbf{q}$ below 0 dB are cut off. Therefore, when adjusting the mean, the replica is also cut-off at 0 dB. A simple least squares objective function is used for optimization of the unknown refractivity profile parameter vector $\mathbf{m}$:

$$\phi(\mathbf{m}) = \sum_{i=1}^{N} [p_i(\mathbf{m}) - q_i]^2 = (\mathbf{p} - \mathbf{q})^{\mathrm{T}} (\mathbf{p} - \mathbf{q}). \qquad (2)$$

2. EXPERIMENTAL DATA

Radar and *in situ* validation data were obtained during the Wallops '98 measurement campaign [4] conducted by the Naval Sur-

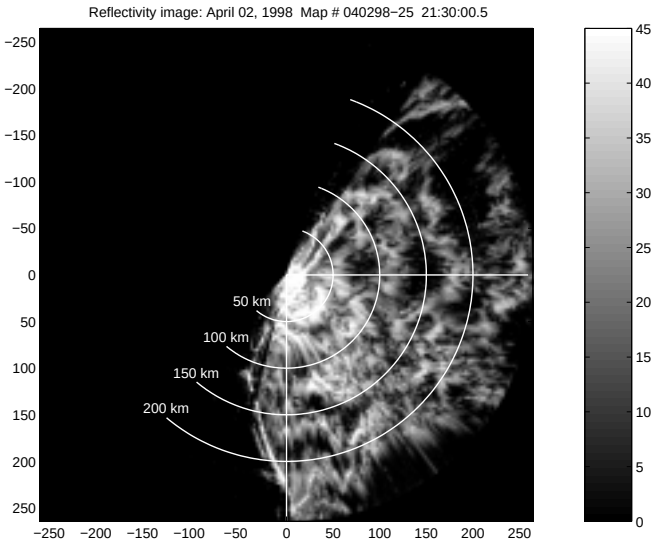

Fig. 2. Clutter map from SPANDAR corresponding to Wallops Run 12.

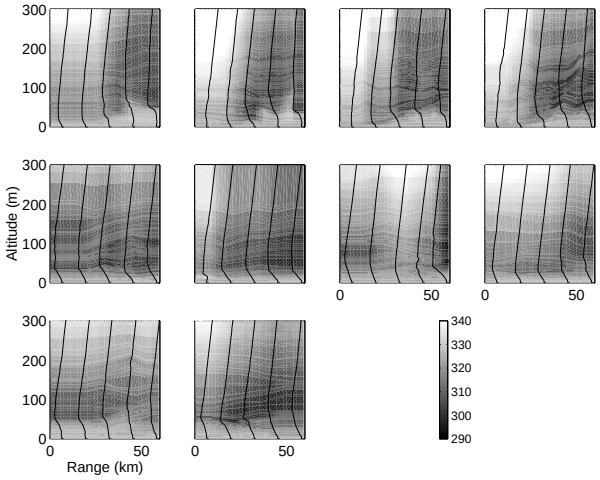

Fig. 3. Refractivity profiles (in M-units) sequenced in time. The first row is observed from 13:47–15:26, middle 17:26–19:15 and bottom 21:00–21:52. All refractivity profiles have the same value at sea level.

face Warfare Center, Dahlgren Division. The data presented here are from the surface-based ducting event that occurred on April 2, 1998. Radar data were obtained using the Space Range Radar (SPANDAR). The antenna height for the SPANDAR is 30.8 meters and clutter maps were taken with the antenna elevation angle set to 0°. All other parameters were set to values given in [4], except pulse width which was set to 2 μsec. A clutter map from the ducting event is shown in Fig. 2.

Meteorological soundings were obtained by an instrumented helicopter provided by the Johns-Hopkins University Applied Physics Laboratory. The helicopter would fly in and out on the 150° radial from a point 4 km due east of the SPANDAR. During the flights, the helicopter would fly a saw-tooth up-and-down pattern. Contour plots of refractivity versus range and height are shown in Fig. 3. Dark lines superimposed on the plot are the modified refractivity profiles. The waveguide can be seen in the first 100 m. The earlier profiles show substantial range dependency.

In Fig. 4 are plotted the envelopes and median values of clutter return data from the SPANDAR. The upper series of plots corresponds to envelopes over different 5-degree sectors from the same clutter map. Plots in the lower series correspond to envelopes over a single 5-degree sector that were obtained at 10-minute intervals. The horizontal broadening of the envelopes with respect to range possibly is explained either by variations in the mean value with respect to range of the parameters, or by random variations in range.

3. INVERSION

The inversion algorithm described in the introduction was initially implemented using a range-independent refractivity model using variations on the vertical structure described in Figure 1. That yielded a mixture of results. We are reasonably certain that most of the poor results stemmed from the range-dependency of the environmental parameters, in particular, that of z_T. This led to shifting the range where features such as clutter rings occur, a behavior that

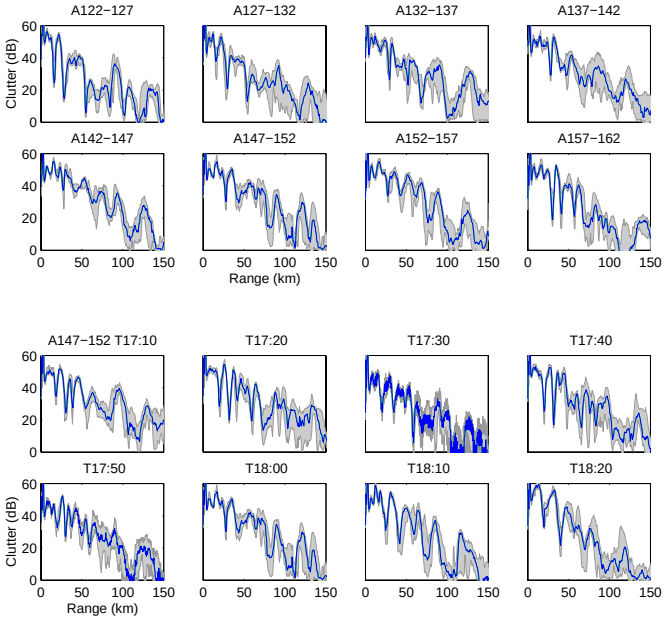

Fig. 4. Clutter return as a function of range for different angles (top) and time (bottom). The shaded area is the envelope of 15 returns in a 5-degree interval and the dark line is the median. In the top figure the 5-degree angle intervals for azimuths centered at 125–160 degrees at time 18:00. In the bottom figure, the time interval is 17:10–18:20.

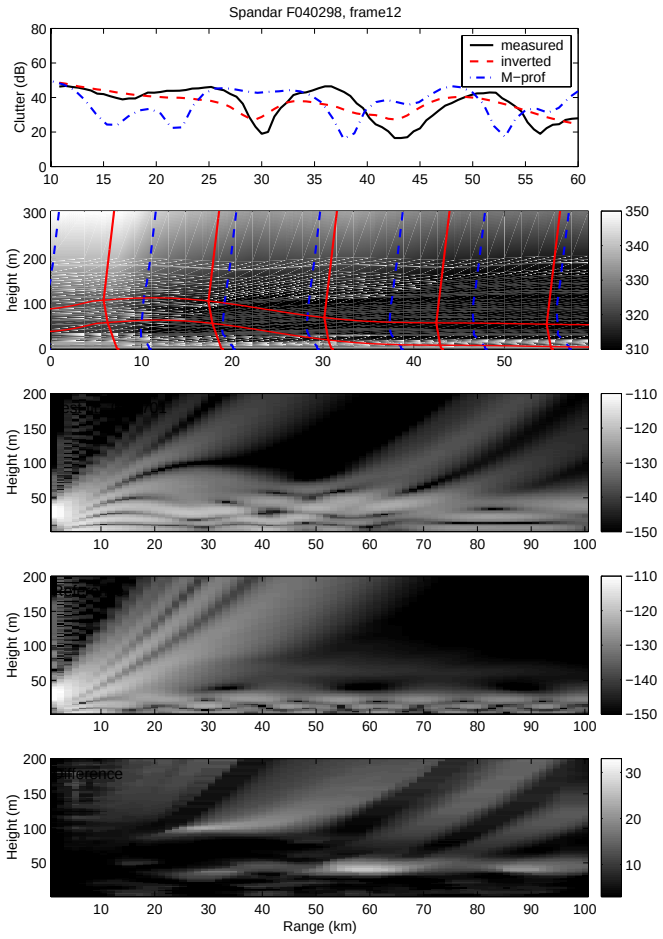

Fig. 5. Refractivity inversion: (a) The clutter return as observed by the radar data (solid), the modeled return using the inverted profile (dash), and the modeled return from helicopter soundings (dash-dot). (b) Observed profiles measured from helicopter (dashed and color-contour) and inverted profiles (solid). (c) Propagation loss coverage diagram corresponding the inverted profiles. (d) Coverage diagram based on helicopter profiles. (e) Difference between coverage diagram d and c.

is problematic when the objective function $f(\cdot)$ is the squared error. In light of that problem, the 5 parameters of $\mathcal{E}$ were augmented by Scripps Institution of Oceanography to include 6 parameters describing the range-dependency of z_T. Those parameters corresponded to coefficients of the six principal components arising from modeling z_T as a Markov process with respect to range. Of course, doing so increased the dimensionality of the problem so an efficient search was implemented via the SAGA (Simulated Annealing / Genetic Algorithm) Code [6, 7] . The implementation of SAGA using the environment description having a total of 11 parameters resulted in improved results. Each SAGA run takes on the order of two hours; we hope to improve on this by an order of magnitude.

A typical example of an inversion is shown in Figure 5. The replica field (dashed) corresponding to the inverted profiles fits some, but not all, of the intensifications and nulls in the observed clutter data (solid). The degree of difference between the observed and estimated clutter can be taken to suggest that not all of the information that is available has been extracted from the clutter. Note, however, the clutter estimate based on the helicopter soundings (dash-dot) itself is an imperfect match to the observed clutter. The propagation loss coverage diagram corresponding to the inverted profiles shows greater trapping in the lower 60 to 70 meters than does the coverage diagram corresponding to the helicopter profiles. The plot of the differences shows errors are generally less than 10 dB within the duct, a region of large errors in the vicinity of the top of the duct (due to the differenced in the height of the duct), and differences of 0 to 25 dB in the "blind zone" the region above the duct at extended ranges.

4. SUMMARY

The work on inferring refractivity parameters is in its infancy. Presumably there is an upper bound on just how much information can be extracted from the clutter; it is surely state-dependent and may only be possible to determine after a parameterization has been specified. Whatever the bound is, however, approaching the bound requires very good fits between observations and optimal replica fields. Understanding the sensitivity of clutter to the variations of parameters is a step in that direction.

5. REFERENCES

[1] Gossard, E.E. and R.G. Strauch, *Radar Observations of Clear Air and Clouds*, Elsevier, 1983.

[2] Krolik, J.L. and J. Tabrikain, Tropospheric refractivity estimation using radar clutter from the sea surface, *Proc. 1997 Battlespace Atmospherics Conference*, SPAWAR Systems Command Tech. Rep. 2989, pp. 635-642, March, 1998

[3] Krolik, J.L., J. Tabrikian, S. Vasudevan and L.T. Rogers, Using radar sea clutter to estimate refractivity profiles associated with the capping inversion of the marine atmospheric boundary layer, *Proc. of IEEE 1999 International Geoscience and Remote Sensing Symposium, Hamburg, Germany*, 28 June - 2 July, 1999

[4] L.T. Rogers, C.P. Hattan, J.K. Stapleton, "Estimating evaporation duct heights from radar sea clutter," *Radio Science*,35(4), pp. 955-966, Jul.-Aug., 2000.

[5] A.E. Barrios, "A terrain parabolic equation model for propagation in the troposphere," *IEEE Trans. Antennas Propagat.*, vol. 42, pp. 90–98, Jan. 1994.

[6] P. Gerstoft, "SAGA Users guide 2.0, an inversion software package," SACLANT Undersea Research Centre, SM-333, 1997. http://www.mpl.ucsd.edu/people/gerstoft/saga.

[7] P. Gerstoft, D.F. Gingras, L.T. Rogers and W.S. Hodgkiss, "Estimation or radio refractivity structure using matched field array processing," *IEEE Trans. antenna Propagat.* , 48, pp. 345–356, Mar. 2000.